

EFFECTS OF BOUNDARY LOCATION ON THE FINITE ELEMENT PREDICTIONS FOR LARGE OPENINGS IN ROCK

M. Abdel Meguid, Graduate student, University of Western Ontario, London, Ontario
R.K. Rowe, Professor of Geotechnical Engineering, Queens University, Kingston, Ontario
K.Y. Lo, Emeritus Professor and Director, Geotechnical Research Centre
University of Western Ontario, London, Ontario

ABSTRACT

A 3D elasto-plastic finite element model that is suitable to analyze the short-term stability of tunnels in weak rock is used to study the effects of rigid boundary locations on the finite element predictions. Emphasis was placed on the effect of boundary location on displacements at the tunnel face, crown and springline as well as on the development of plastic zone around the opening. The analysis focuses on the case of an unlined tunnel constructed in stress and geologic environments prevalent in shales in Southern Ontario. The results are presented for different anisotropic stress conditions. Recommendations for selecting reasonable boundary locations for similar conditions are presented.

RESUME

Un modèle de l'élément fini élastoplastique de 3D qui est convenable d'analyser la stabilité à court terme des tunnels dans la roche molle est utilisé pour étudier les effets des emplacements limites rigides sur les prédictions des éléments finis. L'accentuation a été placée sur l'effet de l'emplacement limite sur les déplacements au parement, en clé et en piedroits du tunnel aussi bien que sur le développement de zone plastique autour de l'ouverture. L'analyse se concentre sur le cas d'un tunnel sans revêtement construit dans les étages de contraintes et environnements géologiques actuels dans les schistes de l'Ontario du sud. Les résultats sont présentés pour les conditions différentes en contrainte anisotrope. Recommandations pour sélectionner des locations limites raisonnables pour les conditions semblables sont présentées.

1. INTRODUCTION

In a typical 3D finite element analysis, the mesh should be selected such that location of lateral boundaries would not significantly influence the finite element predictions. The mesh should also be fine enough to provide details where information is needed. Satisfying these criteria and keeping the problem size manageable is a challenging task for the 3D analysis of tunnels. This is particularly true for the case of modeling large opening in weak rock subjected to high in-situ horizontal stresses ($K_0 > 1$) where high displacements are expected near the tunnel springline.

In the present study, a 3D elasto-plastic finite element model that is suitable for analyzing the short-term stability of tunnels in weak rock was used to investigate the effect of the mesh size on the finite element results. A parametric study was conducted on a tunnel constructed in Queenston Shale with geometrical conditions similar to those considered for Sir Adam Beck Niagara Generating Station Number 3 (SABNG No. 3) project. Four different mesh sizes were examined based on the distance from the tunnel centerline to the rigid boundaries. The in-situ horizontal stress (K_0) was varied and the mesh size effect on the displacement and the plastic zone development around the tunnel circumference was investigated.

In order to investigate the effects of the rock mass strength on the predicted results, the strength was reduced gradually. Four cases were examined

representing a range of rock mass quality from good to poor quality rock mass with ratios of rock mass strength to in situ stress (σ_{cm}/p_o) of 3.0, 1.4, 1.0 and 0.8 respectively. The in situ stress is represented by

$$p_o = \frac{\sigma_v + \sigma_h}{2}$$

Where σ_v and σ_h are the vertical and horizontal stresses respectively.

The results are presented for different stress anisotropic conditions. Recommendations for selecting reasonable boundary locations for similar conditions without affecting the finite element predictions are given.

2. ROCK MASS PARAMETERS

For the design of Sir Adam Beck Niagara Generating Station Number 3 (SABNG No. 3) project (Niagara Falls, Ontario), a tunnel of approximately 13 m diameter and 10 km long is required. The tunnel will be constructed in Queenston Shale at a depth of about 200 m from ground surface to the tunnel centerline. Rock formations in this region are characterized by high initial horizontal stresses. Their magnitudes and directions may vary according to local topographic conditions.

The elastic deformational behavior of shales is essentially orthotropic and may be described by five different parameters. Solutions for stresses and displacements



using these parameters for a circular tunnel have been reported (Hefny and Lo 1999). The Anisotropic parameters have been presented in Lo and Hefny (1993). While it is possible to input these parameters into the three-dimensional analysis, it was decided to simplify the material property input so as to capture the essence of the 3D solutions. A representative set of rock parameters used in the analysis is shown in Table 1.

Table 1. Rock Mass Parameters

Rock parameters	
Young's Modulus (E)	15800 MPa
Poisson's ratio (ν)	0.30
Uniaxial compressive strength:	
- Intact rock (σ_{ci})	37 MPa
- Rock mass (σ_{cm})	37 - 5 MPa
Cohesion (c')	9 - 2.5 MPa
Friction angle (ϕ')	38°
Initial stress ratio (K_0)	1 - 5
Unit weight (γ)	26 kN/m ³

The uniaxial compressive strength of the rock mass is related to the Mohr-Coulomb parameters by the relationship (Hoek *et al.* 1995)

$$s_{cm} = \frac{2c \cos \phi}{1 - \sin \phi}$$

Where, c and ϕ are the cohesion and angle of internal friction respectively.

3. METHOD OF ANALYSIS

The analyses are performed using three-dimensional (3D) elasto-plastic finite element computer program developed based on the library of routines published by Smith and Griffiths (1998) employing the following aspects:

3.1 Full 3D Analysis

In this study, the rock mass is modeled using 20-noded brick elements. The element performance has been checked against simple cases where closed-form solutions exist for comparison, including problems of beam bending, open excavations and underground tunnels. Details of the problems and solutions are given elsewhere (Abdel-Meguid 2001)

3.2 Varied Construction Sequences

Material is removed at several stages so that, for the non-linear analyses, the final stress data is appropriate to the sequence of excavation that would be performed. This process must be conducted in such a way that equilibrium is maintained in the rock elements around the tunnel. Element removal was carried out using procedure

described by Brown and Booker (1985). Initially, the ground is stressed by its own weight. For each excavation stage, the geometry is modified and a new stiffness matrix and load vector is formed. The loads are removed in increments and the nonlinear equations were solved using a modified Newton-Raphson technique. A full integration scheme (27 integration points) has been used in the present analysis.

3.3 Material Non-linearity

It is assumed that the onset of plastic failure of the rock mass is defined by the Mohr-Coulomb criterion. In 3D principal stress space the failure surface associated with the Mohr-Coulomb is an irregular hexagon pyramid with its axis coinciding with the hydrostatic axis as shown in Figure 1. The presence of corners at $\theta = \pm 30^\circ$ creates a non-continuous and non-differentiable failure surface. In the present study, the smoothing algorithm suggested by Smith and Griffiths (1998) is adopted, whereby a smooth surface is substituted in the corners when (see Figure 1).

$$|\sin^{-1} \theta| > 0.492424 \quad (\theta = 29.5^\circ).$$

In this region, the surfaces are evaluated explicitly with either $\theta = 30^\circ$ or $\theta = -30^\circ$ giving a circular surface over a small arc. Different assumptions can be made, but no numerical difficulties have been encountered with the above scheme.

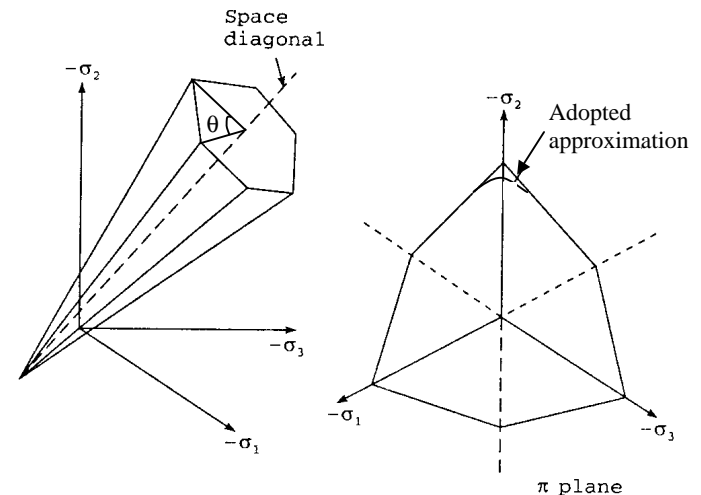


Figure 1. Mohr-Coulomb Failure Criterion in the principal stress space

3.4 Solution Algorithm

Two main types of solution procedure can be adopted to model material non-linearity. The first approach involves "constant stiffness" where the global stiffness matrix is formed once only. For this approach, there are two popular methods of redistributing stresses that lie outside the failure surface, namely, initial stress method and viscoplasticity (Zienkiewicz and Corneau 1974). The saving in computer time enjoyed from only having to operate on one global stiffness matrix is offset by added



iterations as failure is approached. Less iterations per load step are required if the second approach, the “tangent” stiffness method is adopted. The global stiffness matrix is reformed occasionally to account for the reduction in stiffness of the material as failure is approached.

For 3D analysis, reforming and factorizing the global stiffness matrix is computationally very costly and, therefore, a simple viscoplastic algorithm with a modified Newton-Raphson iterative scheme is used in the present study.

3.5 Pre and Post Processing

The task of generating finite element meshes in three dimensions is not trivial. Computer programs that generate the mesh, number the nodes and elements are essential and indeed a number of such programs are commercially available. The graphical interface program GID (GID 1999) was used to generate the finite element mesh and to interpret the results of the 3D analyses.

4. ANALYSIS DETAILS

In order to investigate the effect of the mesh boundary location on the finite element results, the excavated length of the tunnel was fixed at a distance of 5 times the tunnel diameter, 5D. The rigid boundaries were located at equal distance from the tunnel face, springline and invert. Four distances, namely 4D, 5D, 7D and 10D were examined. Mesh arrangement and rigid boundary locations for the cases are shown in Figures 2 to 5 respectively.

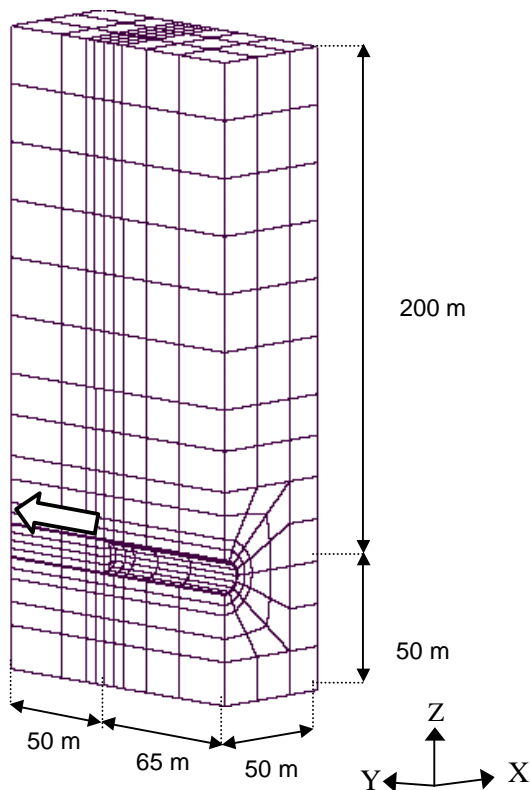


Figure 2. Three-dimensional mesh with rigid boundary distance of 4D

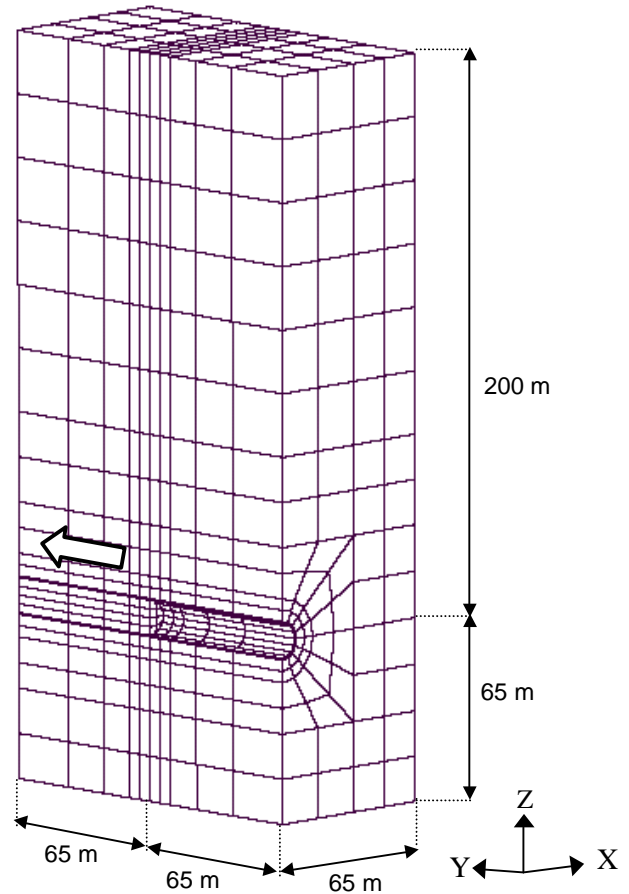


Figure 3. Three-dimensional mesh with rigid boundary distance of (5D)

Loads resulted from the tunnel excavation were removed in 10 increments and convergence was considered to have occurred when the stresses at all gauss points satisfied the failure criterion to within a tolerance of 0.1%.

For the full-scale model of tunneling problem it is necessary to prescribe displacement conditions on the outer boundaries of the problem domain. Referring to Figures 2 to 5, nodes along the vertical boundaries may translate freely along the boundaries but are fixed against displacements normal to these boundaries. The nodes at the base are fixed against displacements in both directions.

In order to investigate the effects of the rock mass strength on tunnel stability and deformation, the strength was reduced gradually by reducing the cohesion (c'). Five cases were examined representing a range of rock mass quality from good to poor quality rock mass using $c' = 9, 4.5, 3.5$ and 2.5 MPa. These values correspond to a ratio of rock mass strength to in situ stress (σ_{cm}/p_0) of about 3.0, 1.4, 1.0 and 0.8 respectively, where the in situ stress is represented by

$$p_o = \frac{\sigma_v + \sigma_h}{2}$$

Where σ_v and σ_h are the vertical and horizontal stresses respectively.

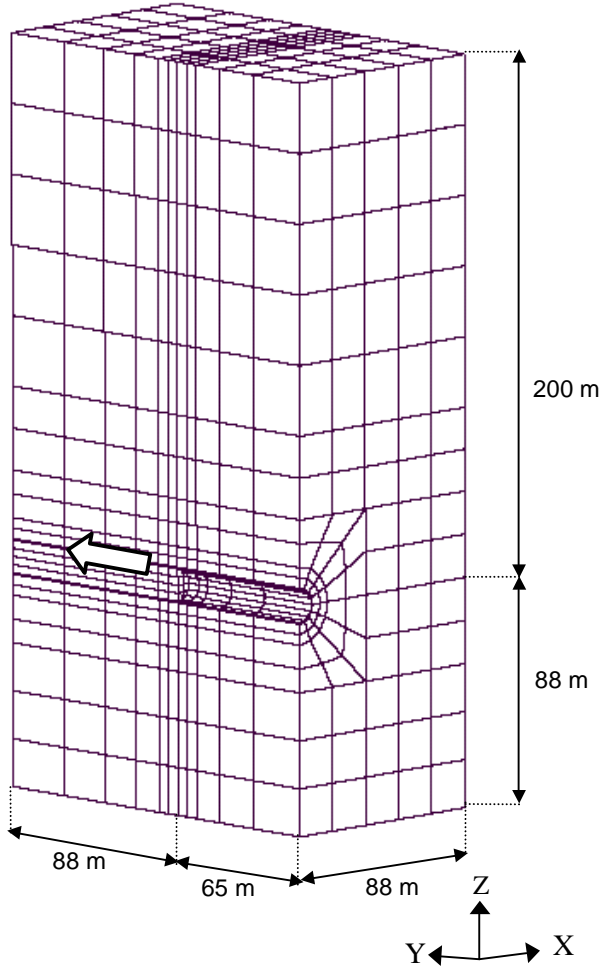


Figure 4. Three-dimensional mesh with rigid boundary distance of (7D)

Displacements at springline for low quality rock, (σ_{cm}/p_o) of 0.8 and 1.1, are shown in Figures 6a and 6b, respectively, for different boundary locations and stress anisotropy. It was observed that displacement generally increased with increasing the earth pressure coefficient (K_o) and decreasing rock mass strength.

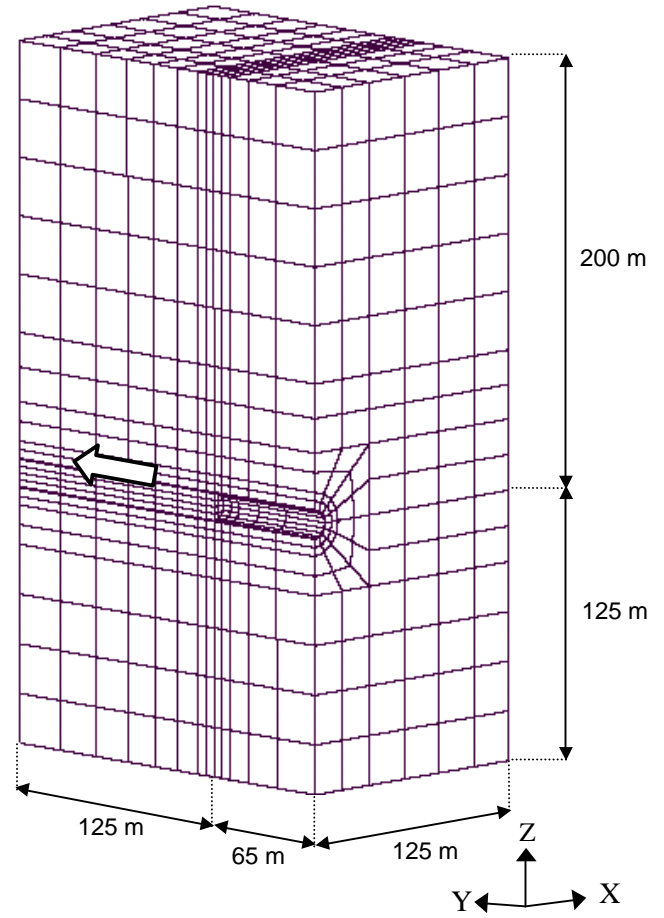


Figure 5. Three-dimensional mesh with rigid boundary distance of (10D)

5. RESULTS OF TUNNEL ANALYSES

5.1 Tunnel Deformation

Results of the tunnel deformation are presented by plotting the displacements at the crown and springline for different mesh sizes and. Displacements are represented in dimensionless form

$$\Omega = \frac{uE}{ap_o}$$

Where E , a , and p_o are, respectively, the elastic modulus, tunnel radius and the in situ stress.

For low quality rock ($\sigma_{cm}/p_o = 0.8$), the horizontal displacement at springline increased by about 12% for $K_o = 5$ with increasing the location of the rigid boundary from 4D to 10D as shown in Figure 6a for. A difference of about 9% was found for the case of $\sigma_{cm}/p_o = 1.1$ and $K_o = 5$ as shown in Figure 6b. No significant change in springline deformation due to moving the boundary from 4D to 10D was calculated for K_o of 1 and 3.

Similar observation was made for the case of high quality rock mass where increase in springline displacement of about 6% was calculated for $K_o = 5$ (Figure 7a). A small increase of about 3% was found for $\sigma_{cm}/p_o = 3.0$.



It was also observed that at a distance of 7D, the displacement predictions at the tunnel springline were very similar to those obtained for a distance of 10D. This suggests that a satisfactory displacement results may be obtained by moving the finite element mesh boundaries to a distance of 7D.

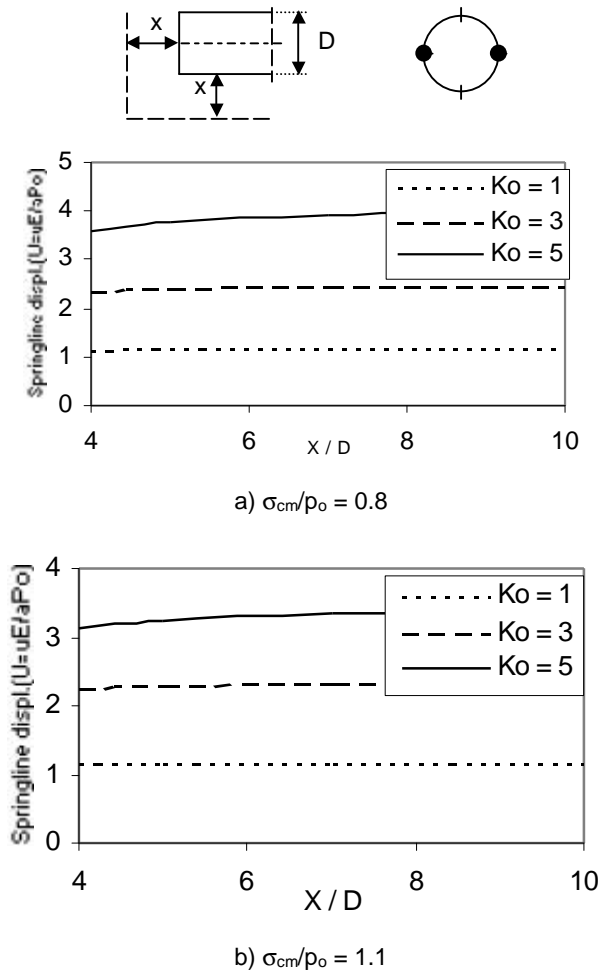


Figure 6. Horizontal displacement at springline for low quality rock mass

Displacement at the face centre was also examined as shown in Figures 8 and 9 for the cases of low and high quality rock respectively. The different mesh boundary locations had an insignificant effect on these displacements. This finding suggests that the displacement results at the tunnel face is not sensitive to the increased extent of the mesh boundary from 4D to 10D and, therefore, boundary near the tunnel face may be kept at a distance less than 10D without affecting the finite element predictions.

At the tunnel crown, (Figures 10 and 11) it was found that as the location of the mesh boundary increased, the vertical displacement decreased for all values of K_0 examined. As the rock mass strength increased outward

displacement at the crown was found and only at a distance of greater than or equal to 7D did the mesh start to capture the change in direction (Figure 11a).

Although the crown displacement was generally small, the change in the displacement was found to range from 10 to 38% with increasing the distance to the rigid boundary location from 4D to 10D for the case of $\sigma_{cm}/\rho_o = 0.8$ and $K_0 = 5$.

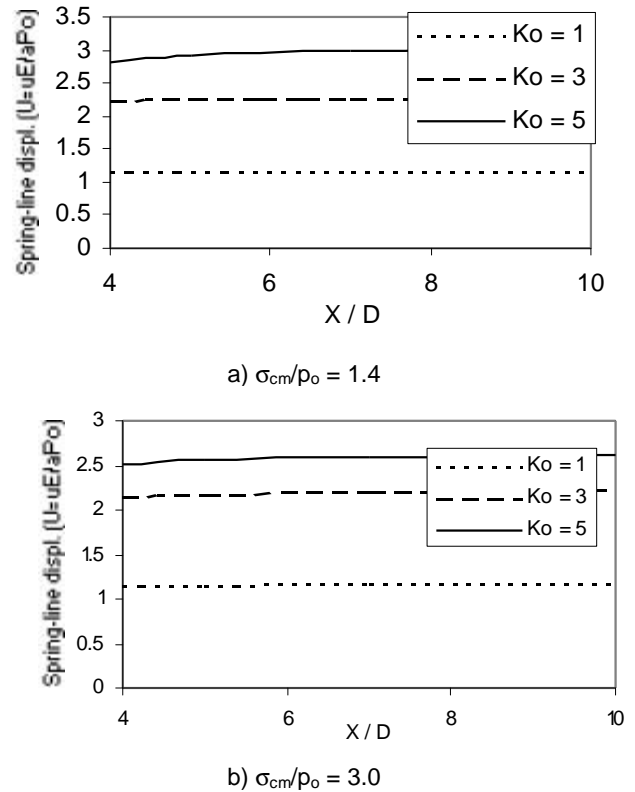


Figure 7. Horizontal displacement at springline for high quality rock mass

5.2 Plastic Zone Development

In order to simplify the identification and 3D plotting of plastic zone, elements with several (more than 9) plastic Gauss points are considered to become plastic and the number of these plastic elements is plotted in Figure 12 as a function of the distance to the mesh boundaries for different rock mass strengths. A plastic zone was only developed for the cases of $K_0 = 3$ and 5. As the rock mass strength increased the number of elements with plastic Gauss points generally decreased. It was also observed that this number of elements increased with increasing mesh distance to the rigid boundary location. Satisfactory displacement results were found at a distance of about 7D at the tunnel face, invert and springline for the range of rock properties used in this study.



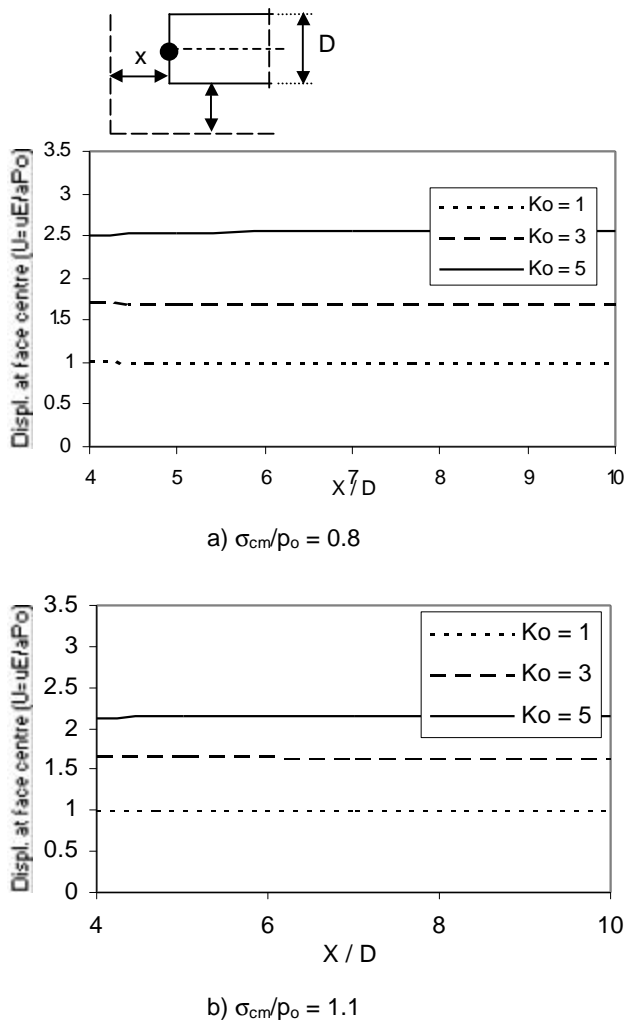


Figure 8. Horizontal displacement at face centre for low quality rock

5.3 Comparison Between Different Meshes

Based on the 3D analysis, a comparison between displacement results obtained using different meshes is summarized in Table 2. Displacements were compared with that calculated using $\sigma_{cm}/p_o = 0.8$ for the case of rigid boundary located at $10D$ and $K_o = 5$. The results obtained using a distance of $4D$ is corresponding to a less number of nodes and therefore, less computational effort. However, the springline displacement was underestimated by 12% and crown displacement was overestimated by 38%.

Computer processing times for the case of $\sigma_{cm}/p_o = 0.8$ and $K_o = 5$ using different meshes is summarized in Table 2. Saving in computational effort (about 75%) coupled with reasonable accuracy was found for the case of distance to mesh boundary = $7D$.

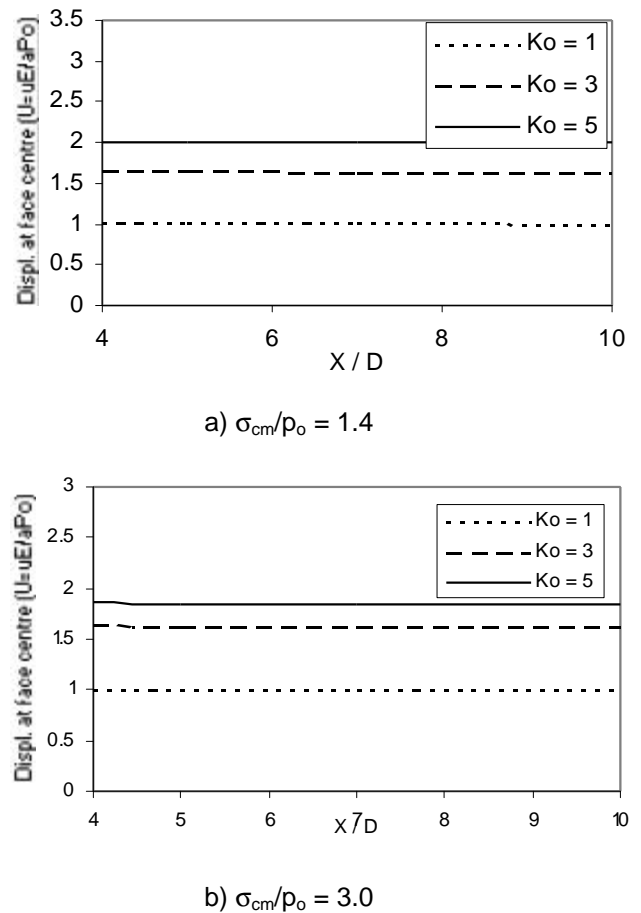


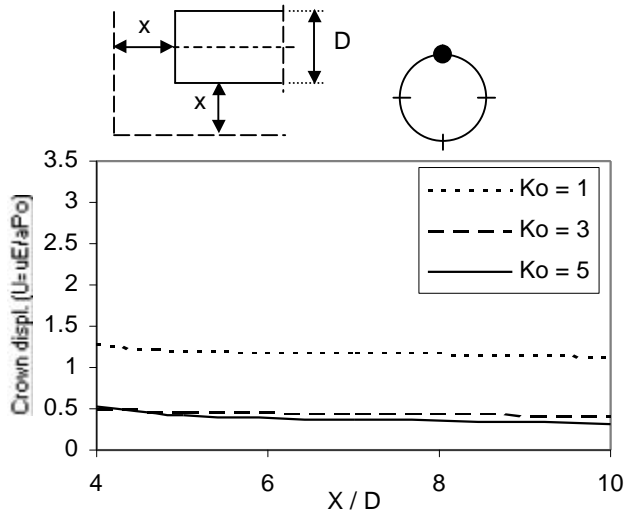
Figure 9. Horizontal displacement at face centre for high quality rock

Table 2. Comparison between results using different meshes

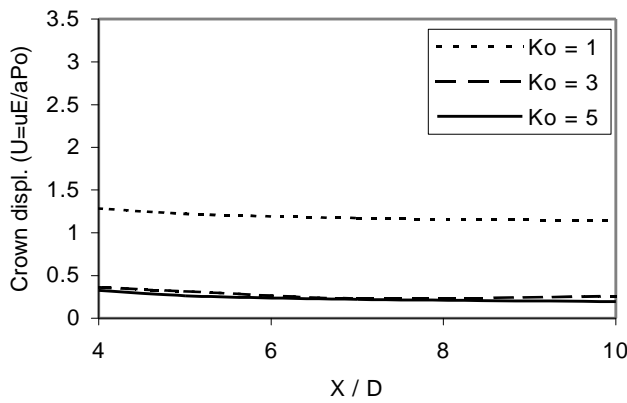
Distance to mesh boundary	4D	5D	7D	10D
No of Nodes	3709	4885	6033	8243
No of Element	711	960	1210	1690
% Difference in spring line displacement *	12	6	2	0
% Difference in crown displacement *	-38	-25	-10	0
Computing time (min.)	20	40	110	195

*Compared with the calculated displacement using $\sigma_{cm}/p_o = 0.8$ for the case of rigid boundary located at $10D$ and $K_o = 5$.





a) $\sigma_{cm}/p_o = 0.8$



b) $\sigma_{cm}/p_o = 1.1$

Figure 10. Vertical displacement at crown for low quality rock

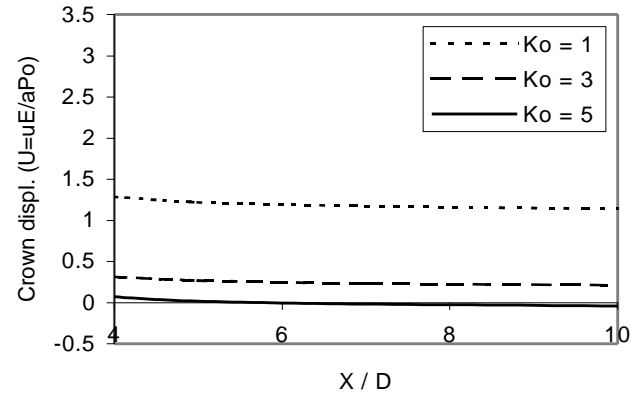
6.0 COMPUTING RESOURCES

All the mesh-development, 2D analysis, simple 3D analysis runs and post-processing were performed on PC (750 MHz with 256 Mb memory). The runs for full analysis were performed on IBM Workstation 44P model 270, two-way CPU with 275 MH and 1 GB memory.

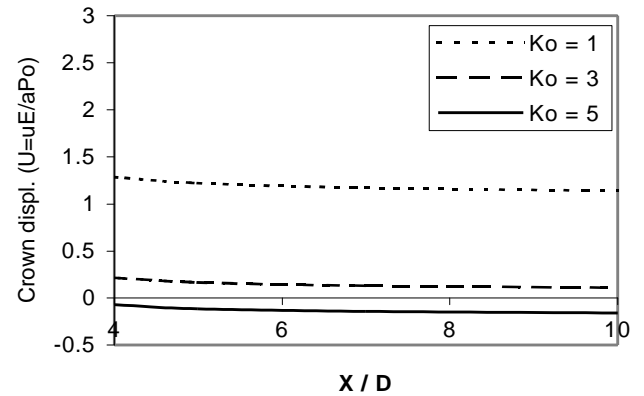
7.0 CONCLUSIONS

Three-dimensional elasto-plastic finite element method was used to simulate the construction of a large diameter tunnel in weak rock subjected to high horizontal stresses.

The rock mass strength was reduced gradually by reducing the cohesion (c). Five cases were examined representing a range of rock mass quality from good to poor quality rock mass. The rigid boundaries were located at equal distance from the tunnel face, springline and invert. This distance was increased in four steps namely 4D, 5D, 7D and 10D.



a) $\sigma_{cm}/p_o = 1.4$



a) $\sigma_{cm}/p_o = 3.0$

Figure 11. Vertical displacement at crown for high quality rock

The analysis allowed the calculation of the tunnel deformation and the identification of plastic zone development around the face.

A satisfactory displacement results was obtained by moving the finite element mesh boundaries to a distance of 7D. Substantial savings in computational effort with acceptable accuracy may be obtained.

It may be concluded that the mesh boundary location is important factor in the finite element predictions for tunnels subjected to high horizontal stresses. The required boundary extent depends on the rock mass strength and the in-situ horizontal stresses. It is recommended that, for the range of $5 > K_o > 3$, the rigid

boundary may be located at a distance of about 7D without acceptable accuracy for the finite element predictions. For the range of $K_o < 3$, a distance of 5D is sufficient to provide an acceptable predictions for displacement field as well as plastic zone development around tunnels in rock.

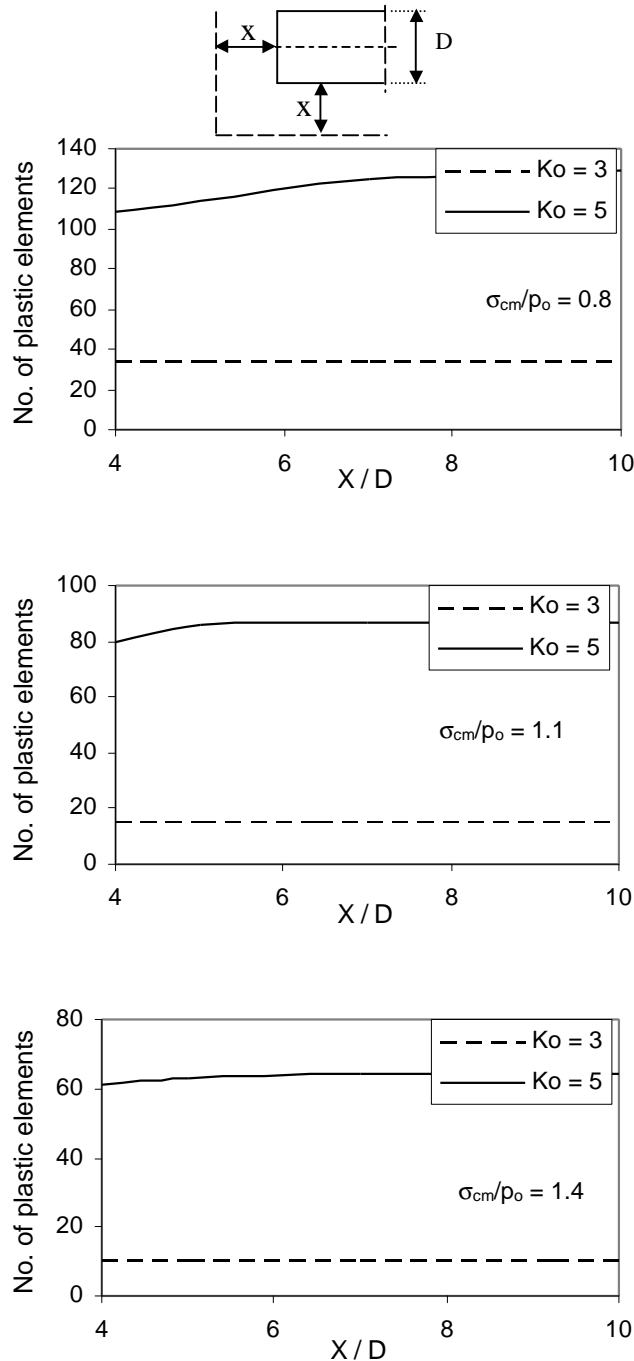


Figure 12. Elements with plastic gauss points for different boundary distances

8.0 ACKNOWLEDGEMENTS

This research is supported by the Natural Sciences and Engineering Research Council of Canada (NSERC). Support in the form of NSERC Post Graduate Scholarship (PGSB) and Ontario Government Scholarship in Science and Technology (OGSST) are also acknowledged.

9.0 REFERENCES

- Abdel-Meguid, M., 2001. Some three-dimensional aspects of tunneling. Ph.D. Thesis. University of Western Ontario. (In preparation).
- Brown, P. T. and Booker, J. R. 1985. Finite element analysis of excavations. *Computers and Geotechnics*, 1(3): 207-220
- GID, version 6.0, 1999. International Centre for Numerical Methods in Engineering. Barcelona, Spain.
- Hefny, A.M. and Lo, K.Y. 1999. Analytical solutions for stresses and displacements around tunnels driven in cross-anisotropic rocks. *International Journal for Numerical and Analytical Methods in Geomechanics*, Vol. 23, No. 2, pp. 161-177.
- Hoek, E., Kaiser, P.K. and Bawden, W.F. 1995. Support of underground excavations in hard rock. Rotterdam, Balkema.
- Lo, K.Y. and Hefny, A. 1993. The evaluation of in-situ stresses by hydraulic fracturing tests in Anisotropic rocks with mixed-mode fractures. *Canadian Tunneling Journal*, pp. 59-73.
- Lo, K.Y., Lukajic, B. and Ogawa, T. 1984. Interpretation of stress-displacement measurements. *Proceedings of session sponsored by ASCE, Geotech. Atlanta, GA*, 128-155.
- Lo, K.Y. and Yuen, M.K. 1981. Design of tunnel lining in rock for long term time effects. *Canadian Geotechnical Journal*, 18(1): 24-39.
- Lo, K.Y., Ogawa, T., Sekiguchi, K. and Rowe, R.K. 1992. Large deformation and face instability in tunneling through thick fault zones. *Canadian Tunneling Journal*, pp. 77-96.
- Smith I.M. and Griffiths D.V. 1998. Programming the finite element method. Third edition. John Wiley, London.
- Zienkiewicz, O. C. and Corneau, I. C., 1974. viscoplasticity, plasticity and creep in elastic solids. A unified numerical solution approach. *Int. J. Num. Meth. Eng.*, 8, 821-84.

